

INFLUENCE OF PROCESSING PARAMETERS ON FORMING QUALITY OF NON-CIRCULAR SPINNING

Qinxiang Xia
School of Mechanical & Automotive
Engineering
South China University of Technology
Wushan RD., Tianhe District, China
meqxxia@scut.edu.cn

Zhouyi Lai
Electromechanic Engineering College
Shenzhen Institute of Information Technology
Shenzhen
Longxiang Avenue, Longgang District, China
laizhouyi@sohu.com

Juxin Qu
School of Mechanical & Automotive
Engineering
South China University of Technology
Wushan RD., Tianhe District, China
qujuxin@126.com

Cheng Xiu-quan
School of Aircraft Maintenance Engineering
Guangzhou Civil Aviation College
Jichang road, Xiangyun West Street, China
chengxiuquan@caac.net

ABSTRACT

Processing parameters have great influence on forming quality of non-circular spinning. Finite element simulation model of non-circular spinning for the three straight-edge round-corner cross-section (TSRC) hollow-part was established. Variation rules of thickness and springback of TSRC spun workpiece under different processing parameters were obtained by means of orthogonal test as well as the software MSC.MARC. The results show that the influences of the relative clearance ΔC and the feed ratio of roller f_z on the maximum wall thickness thinning ratio δ_r are obvious, and the influences of n and D_r are slight; the influences of the nose radius of roller r_p on the springback angle $\Delta\alpha$ is the most obvious, and the influences of ΔC and D_r are slight.

Keywords: non-circular spinning, processing parameters, forming quality.

1 INTRODUCTION

Traditional definition of the metal spinning technology is that a continuous and local plastic forming occurs in the blank to form an axis-symmetrical hollow part by means of roller feeding and mandrel rotational movements (Wong et al. 2003). In recent years, a new spinning technology of hollow part with non-circular cross-section is developed (Awiszus 2005). It has the characteristics of high flexibility, high productivity and lost productive cost, and can be used to produce various parts with complex shapes and sizes (Music et al. 2005). Lots of researches proved that comparing with conventional spinning, non-circular spinning has different characteristics in distributions of wall thickness, springback and spinning force, etc (Arai 2005, Awiszus 2011). Awiszus et al. (2005) carried out feasibility test of hollow part with triangle cross-section by a simple spinning device where the radial force provided by spring was taken for constant. The result showed that the thickness thinning rate around junction of bottom and sidewall reached 40%. Cheng et al. (2011) analyzed the thickness distribution of spun hollow part with four arc-typed cross-section. The result showed that the thickness thinning increases with decreasing in the axial feed of roller f_z and the nose radius of roller r_p . To study the influence of the main processing parameters on the forming quality of non-circular spinning, the hollow parts with three straight-edge round-corner cross-section (TSRC) which has the typical non-circular feature had been selected as the researched object. The effects of the main processing parameters, such as the roller diameter, roller nose radius, relative clearance between the

roller and mandrel, spindle rotational speed and roller feed rate, on the forming quality were obtained based on numerical simulation combining with orthogonal experimental design.

2 MODEL CONSTRUCTION AND PROGRAM DESIGN

2.1 Finite Element Analysis Model

To obtain the influencing factors on the spun quality of non-circular spinning, the TSRC hollow part was selected as the study object (as shown in Figure 1). The part was divided into the straight-side and filleted-corner along the tangential direction, and the bottom-corner, side-wall and opening-end along the generatrix direction. H refers to the height of the part.

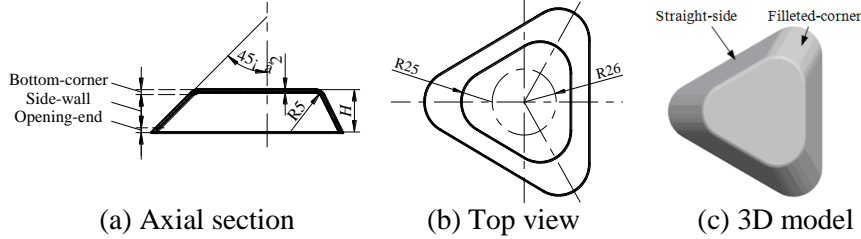


Figure 1: Hollow parts with three straight-edge round-corner cross-section.

As shown in Figure 2, the single pass deep-drawing spinning as stated by Xia *et al.* (2005) with a flat sheet metal blank was adopted, where D_r , r_p and β refer to the diameter, nose radius and installation angle of roller, h refers to the forming height during spinning. The blank material was cold rolled steel sheet SPCC with thickness $t_0=2$ mm.

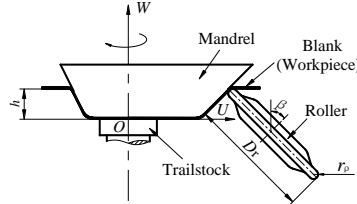


Figure 2: Single pass deep-drawing spinning.

The software Msc. MARC was used to simulate the spinning process. The blank is defined as the elastic-plastic deformation body, the hexahedral element with eight nodes was adopted for the blank meshing. The No.7 element used for large metal deformation was adopted, which is the default element type of software MSC.MARC. The blank is discretized into 8-node hexahedral elements with double layers along the thickness direction (Xia *et al.* 2008), the ratio of the longest side to the shortest side of meshes of all elements is less than 3. The total number of elements is 7282 and the total number of nodes is 14564 in the established finite element analysis (FEA) model (as shown in Fig. 3). The spinning mandrel, tailstock and roller were defined as rigid bodies. The Coulomb friction model is used for the contact between the roller and the blank, the friction coefficient is 0.05 (Liu 2007).

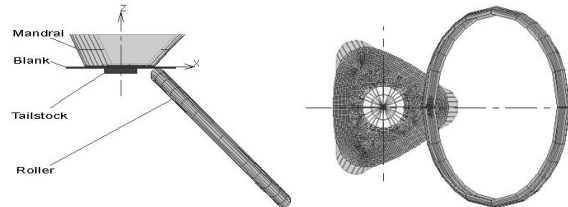


Figure 3 : FEA model of non-circular spinning of TSRC hollow part.

The blank material is SPCC. The mechanical properties listed in Table 1 were obtained by the uniaxial tensile test (Xia *et al.* 2011).

Table 1: Mechanical properties of blank (Xia *et al.* 2011).

Young's modulus E (GPa)	Poisson's rate μ	Stress yield σ_s (MPa)	Tensile strength σ_b (MPa)	Hardening Index n	Strengthening coefficient K
182.9	0.26	218	327	0.22	571.8

2.2 Orthogonal Test Design

As stated by Xia *et al.* (2005), processing parameters influencing the spun quality mainly includes the following items: roller diameter D_r , nose radius of roller r_ρ , relative clearance between mandrel and roller ΔC ($\Delta C = 100\% (C-t_0)/t_0$, where C is the clearance between mandrel and roller, t_0 is the blank thickness), rotational speed of mandrel n and feed ratio of roller along axial direction f_z (as shown in Figure 3). Five different levels were selected for each factor, and the range of each factor level was based on the results of preliminary experiments. The orthogonal array experiment L25 (5^5) for 5 factors and 5 levels was designed. The simulation schemes and results are listed in Table 2.

Table 2: Factors and levels of orthogonal array.

Levels \ Factors	Roller diameter D_r [mm]	Feed ratio f_z [mm/r]	Relative clearance ΔC [%]	Nose radius r_ρ [mm]	Rotational speed of mandrel n [r/min]
1	160	0.3	0	5	25
2	200	0.4	-5	7	45
3	240	0.5	-10	9	60
4	280	0.6	-15	11	80
5	320	0.7	-20	13	108

2.3 Evaluation Targets

Thickness uniformity and springback are the important indexes to evaluate the forming quality of spun parts. As shown in Figure 4, define that δ_t is the maximum wall thickness thinning ratio along the intermediate generatrix direction of filleted-corner I or straight-side II surfaces ($\delta_t = 100\% \times (t_f - t_0)/t_0$, where t_f is the actual wall thickness of spun workpiece); $\Delta\alpha$ is the springback angle ($\Delta\alpha = \alpha - \alpha_0$, where α is the actual half cone angle of spun workpiece and α_0 is the half cone angle of mandrel).

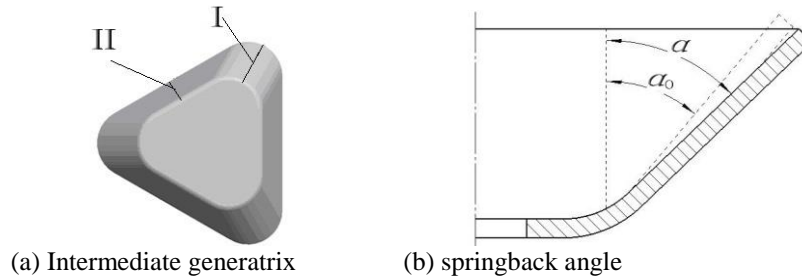


Figure 4: Diagram of evaluation index.

3 SIMULATION RESULTS AND ANALYSIS

3.1 Effect of Five Factors on Maximum Wall Thickness Thinning Ratio

Figure 5 shows the influences of five spinning parameters D_r , r_ρ , ΔC , n and f_z on the maximum wall thickness thinning ratio δ_t , the vertical coordinate is the mean value of the sum of δ_t of all levels in each spinning parameter, which is defined as the result of the evaluation index and obtained by range analysis (Xuan 2011). Figure 6 shows the relationships between the five factors and δ_t .

Figure 5 shows that the variation tendencies of wall thickness thinning both in surfaces I and II are the same, (1) δ_t decreases with the increasing of roller diameter D_r and increases with the increasing of feed ratio of roller f_z . (2) Wall thickness thinning is the most slight when the relative clearance ΔC is -10%, and is the most serious when ΔC is 0; the maximum wall thickness thinning ratio δ_t increases

gradually when ΔC increases from -20% to -10%, while decreases obviously when ΔC increases from -10% to 0. (3) Wall thickness thinning is the most slight when the nose radius of roller R_ρ is 11 mm; δ_t increases gradually when R_ρ increases from 5 mm to 11 mm, while decreases obviously when R_ρ increases from 11 mm to 13 mm. (4) δ_t varies slightly with the variation of rotational speed of mandrel n .

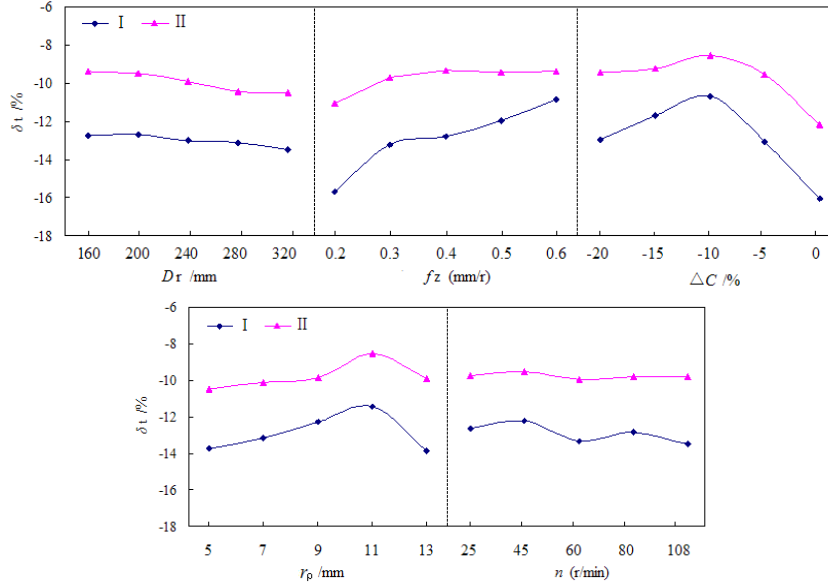


Figure 5: Effects of D_r , r_ρ , ΔC , n and f_z on δ_t .

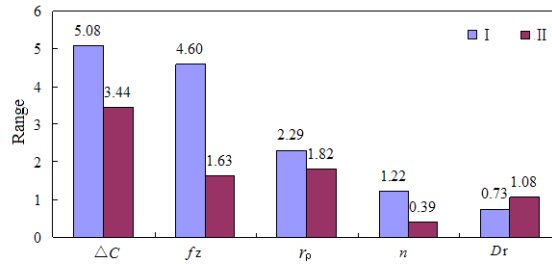


Figure 6: Relationships between D_r , r_ρ , ΔC , n and f_z and δ_t .

Figure 6 shows that the influences of the relative clearance ΔC and the feed ratio of roller f_z on the maximum wall thickness thinning ratio δ_t are obvious, and the influences of n and D_r are slight; the influence sequence on the maximum wall thickness thinning ratio δ_t is relative clearance ΔC , feed ratio of roller f_z , nose radius of roller R_ρ , rotational speed of mandrel n and roller diameter D_r .

3.2 Effect of Five Factors on Springback Angle

Figure 7 shows the influences of five spinning parameters D_r , r_ρ , ΔC , n and f_z on springback angle $\Delta\alpha$, Figure 8 shows the relationships between the five factors and $\Delta\alpha$.

Figure 7 shows that the variation tendencies of springback both in surfaces I and II are almost the same, (1) the springback angle $\Delta\alpha$ varies slightly with the variation of the roller diameter D_r and relative clearance ΔC . (2) $\Delta\alpha$ decreases gradually with the increasing of feed ratio of roller f_z . (3) $\Delta\alpha$ approximately linear increases with the increasing of nose radius r_ρ and rotational speed of mandrel n .

Figure 8 shows that the influences of the nose radius of roller r_ρ on the springback angle $\Delta\alpha$ is the most obvious, and the influences of ΔC and D_r are slight; the influence sequence on the springback angle $\Delta\alpha$ is nose radius of roller r_ρ , rotational speed of mandrel n , feed ratio of roller f_z , roller diameter D_r and relative clearance ΔC .

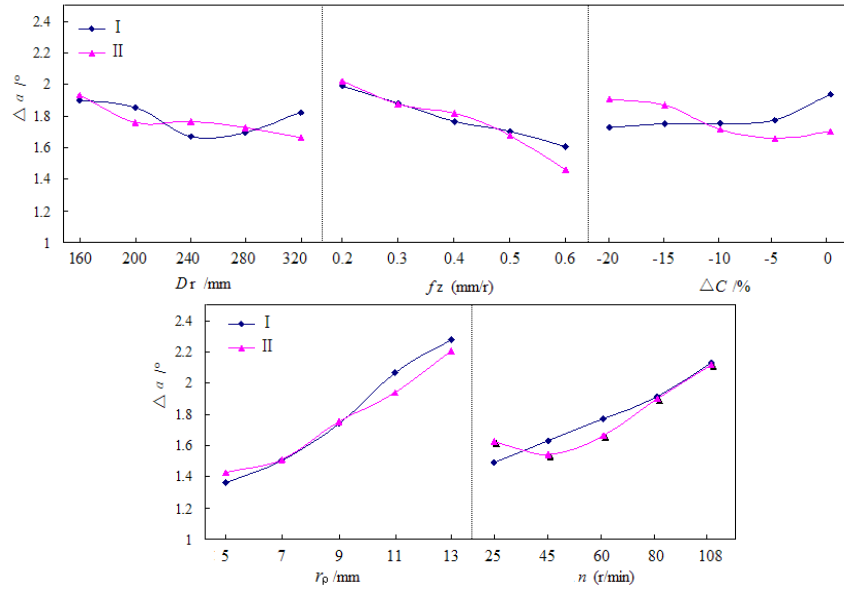


Figure 7: Effects of D_r , r_ρ , ΔC , n on $\Delta\alpha$.

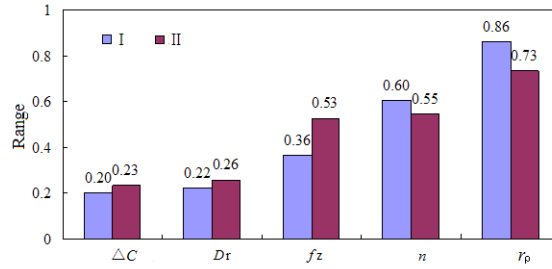
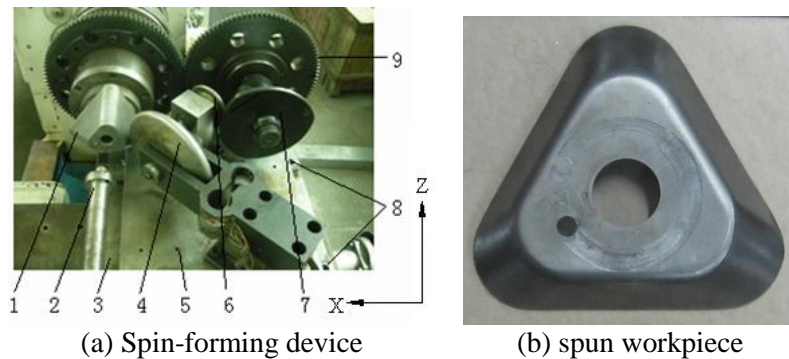


Figure 8: Relationships between D_r , r_ρ , ΔC , n and f_z and $\Delta\alpha$.

4 EXPERIMENT AND ANALYSIS

The experiment was carried out on the HGPX-WSM spinning machine (Xia *et al.* 2006), the processing parameters used for experiment were the same as the numerical simulation scheme one ($D_r=240\text{mm}$, $r_\rho=9\text{mm}$, $\Delta C=0$, $n=45\text{r/min}$ and $f_z=0.3\text{mm/r}$), as listed in Table 2. Figure 9 shows the experiment device (Xia *et al.* 2013) and the spun workpiece formed by the experiment.

Table 3 shows the comparison of experimental and simulation results. It shows that the maximum wall thickness thinning ratio δ_t of experimental result is 13.54%, and the corresponding simulation result is 13.03%. The relative error between two results is only -3.77%, which equals $(13.03\% - 13.54\%) / 13.54\% \times 100\%$. The experimental results conform well with the simulation one. It indicates that the FEA model established in this paper is reasonable and reliable.



(a) Spin-forming device

(b) spun workpiece

Figure 9: Spin-forming device based on profiling driving and spun workpiece (1-Spinning mandrel, 2-Tailstock, 3-Worktable A, 4-Spinning roller, 5-Worktable B, 6-Profiling roller, 7-Profiling mandrel, 8-Guide strip, 9-Gear).

Table 3: Comparison of maximum δ_t between experimental and simulation results.

Simulation/ δ_t [%]	Experiment/ δ_t [%]	Relative error [%]
-13.03	-13.54	-3.77

5 CONCLUSIONS

The influence of main processing parameters on forming quality during non-circular spinning was investigated based on orthogonal experimental design. The conclusions are as follows:

(1) The variation tendencies of maximum wall thickness thinning and springback along the intermediate generatrix direction of filleted-corner or straight-side surfaces are the same.

(2) The maximum wall thickness thinning ratio δ_t decreases with the increasing of roller diameter D_r and increases with the increasing of feed ratio of roller f_z ; δ_t varies slightly with the variation of rotational speed of mandrel n ; the optimum values of the relative clearance ΔC and the nose radius R_ρ exit in view of decreasing the wall thickness thinning.

(3) The springback angle $\Delta\alpha$ increases with the increasing of nose radius r_ρ and rotational speed of mandrel n , but decreases with the increasing of feed ratio of roller f_z ; $\Delta\alpha$ varies slightly with the variation of the roller diameter D_r and the relative clearance ΔC .

(4) The influence sequence on the maximum wall thickness thinning ratio δ_t is relative clearance ΔC , feed ratio of roller f_z , nose radius of roller R_ρ , rotational speed of mandrel n and roller diameter D_r ; and the influence sequence on the springback angle $\Delta\alpha$ is nose radius of roller r_ρ , rotational speed of mandrel n , feed ratio of roller f_z , roller diameter D_r , and relative clearance ΔC .

ACKNOWLEDGMENTS

This research is financially supported by National Natural Science Foundation of China (No.50775076).

REFERENCES

- Arai, H. 2005. Robotic metal spinning-forming asymmetric products using force control. *Proceedings of the 2005 IEEE International Conference on Robotics and Automation*. Barcelona, Spain.
- Awiszus, B. and Meyer, F..2005. Metal spinning of non-circular hollow parts. *Proceedings of the 8th International Conference on Technology of Plasticity*. Verona, Italy.
- Awiszus, B. and S. Hartel. 2011. Numerical simulation of non-circular spinning: a rotationally non-symmetric spinning process. *Production Engineering*, 5:605-612.
- Liu Chun-Ho. 2007. The simulation of the multi-pass and die-less spinning process. *Journal of Materials Processing Technology*, 192-193: 518-524.
- O. Music, J.M. Allwood, K. Kawai. 2009. A review of the mechanics of metal spinning, *Journal of Materials Processing Technology*, 210 (1): 3-23.
- Qinxiang Xia, Susumu Shima, Hidetoshi Kotera, Daifu Yasuhuku. 2005. A study of the one-path deep drawing spinning of cups. *Journal of Materials Processing Technology*, 159:397-400.
- Qinxiang Xia, Peng Zhang, Wu Xiaoyu, Xiuquan Cheng. 2011. Research on distributions of stress and strain during spinning of quadrilateral arc-typed cross-section hollow part. *2011 International Conference on Mechanical, Industrial, and Manufacturing Engineering*. Australia, Melbourne.
- Wong, C.C., T.A. Dean, J. Lin. 2003. A review of spinning, shear forming and flow forming processes. *International Journal of Machine Tools & Manufacture*,43:1419-1435.
- Q.X. Xia, X.Q. Cheng, Y. Hu, F. Ruan: Finite Element Simulation and Experimental investigation on the Forming Forces of 3D Non-axisymmetrical tubes spinning. *International Journal of Mechanical Sciences*, Volume 48, Issue 7, July 2006: P 726-735
- Q.X. Xia, Sh.W. Xie, Y.L. Huo, F. Ruan. Numerical simulation and experimental research on the multi-pass neck-spinning of non-axisymmetric offset tube. *Journal of Materials Processing Technology*, Vol. 206, n 1-3, Sep. 12, 2008, P500-508

- Xia Qinxiang, Lai Zhouyi, Zhan Xinxi, Cheng Xiuquan. 2010. Research on spinning method of hollow part with triangle arc-type cross-section based on profiling driving. *Steel Research International*, 81 (9) :994-997.
- Xia, Q.X., Lai Z.Y., Long Hui, Cheng X.Q.. 2013. A study of the spinning force of hollow parts with triangular cross sections. *The International Journal of Advanced Manufacturing Technology*, 65.
- X.Q. Cheng, X.Y. Wu, Q.X. Xia. 2011. Research on Thickness Distribution of Spun Hollow Part with Four Arc-typed Cross-section. *Proceedings of the 10th International Conference on Technology of Plasticity, ICTP 2011*, Sep. 25-30, Aachen, Germany. P560~563.
- Xuan Wu, Dennis Y.C. Leung. 2011. Optimization of biodiesel production from camelina oil using orthogonal experiment. *Applied Energy*, 88: 3615–3624